# Investigation of crack development in a fairfaced concrete floor

Michael Weiler, Danièle Waldmann

University of Luxemburg, Luxemburg, L-1359

## Abstract

The present work shows the crack behaviour of fairfaced concrete floors and the accurate prediction of cracking. The causes for cracking are various and can be divided into cracking of an early stage concrete and cracking of concrete of a later stage. Here the cracking of the concrete at an early stage due to shrinkage taking into account the strength evolution during hardening, will be analysed. Shrinkage causes a reduction of the structures' volume, it tries to constringe. If the boundary conditions are inconvenient, it may cause cracks. Besides, there are thermal causes based on hydration. As a consequence thereof, the strength of concrete develops in the first days after pouring, too. When the concrete starts to cool down, strains may occur which leads to cracking. For that reason, an experimental investigative program is achieved. With the use of a large climate chamber, in which temperature and humidity can be varied, special specimen with a large surface to volume ratio is stored. An available prognosis software program will give the resulting strengths and internal temperatures at different locations and different instants of time of the investigated elements. These results will be implemented into the finite element models

**Keywords:** Concrete, Crack development, Finite element analysis, shrinkage, strength development

## 1 Introduction

A research project of the Laboratory of Solid Structures of the University of Luxembourg investigates the cracking behaviour of fairfaced and hybrid fibre-reinforced concrete floors, with the screeds serving directly as the final surface, mainly for application in service buildings or in industrial construction. These floors consist of various concrete mixes, which are applied in several layers, and the upper surface has to satisfy serviceability, durability, sustainability and aesthetic requirements. Thus, their behaviour will be similar to the behaviour of industrial floors applied directly on soil, while the border conditions as well as the surface qualities that have to be guaranteed are different. Such structures will present unexpected cracks which can initially be caused by inadequate planning and design or shortcomings in the execution of work. In the absence of those causes, unknown stress conditions of residual stresses or thermal hygric stresses can be at the origin of the observed cracking. All these aspects will be taken into account and will have to be correlated to other factors such as the optimization of the concrete formulations on the basis of the cement used, or the bond properties of the fairfaced concrete screed to the supporting slab under respect of different deformation situations and curing. The study will be mainly executed on the basis of numerical simulations, whereas single results will be controlled by experimental tests. The investigations will be carried out in cooperation with the company Dyckerhoff in Germany.

There are many reasons of cracking of early stage concrete such as thermal stress caused by hydration, strains due to shape change of formwork and hindered shrinkage. Cracking of concrete caused by hindered shrinkage is one of the most important challenge by building a structural component. Here especially specimens with a large volume to surface ratio are involved.

In order to be able to calculate the cracking behaviour of fairfaced concrete floors taking into account shrinkage problems by finite element calculations, the following investigations have been initiated and must be seen as a first step towards the set task.

General reasons for cracking of early stage concrete were researched since years [Wischers & Manns 1972; Kampen 2002]. Thermal stress caused by hydration were investigated in [Thienel &Kustermann 2011; Braasch &Buschmeyer 2006; Li, Nie &Wang 2014; De Schutter 1996 und 2002]. Cracking induced by hindered shrinkage was object of experimental researches [Kronlöf, Leivo & Sipari 1995; Lampropoulos &Dristsos 2011].
One option to avoid or to reduce cracking of a concrete structure is the use of additive and/or fibres. There were investigations [Leemann, Nygaard & Lura 2014] that deal with additives and a range of investigations [Leemann, Nygaard & Lura 2014; Bathia & Gupta 2006; Banthia & Sappakittipakorn 2006; Banthia & Nandakumar 2003; Banthia & Sheng 1996; Yao, Li & Wu 2003; Hsie, Tu & Song 2008] that deal with fibre reinforced concrete. Therein the percentage, material, form and mixture of different fibres were evaluated.
The following paper shows the crack initiation and the crack development of a concrete C20/25 without any kind of additives and fibres. With the help of a special H-shaped concrete specimen cracks caused by hindered shrinkage was visually controlled and documented at precise time steps. The development of material properties such as compressive strength and E-modulus was predicted with the help of a software program called “KINFEST”, the development of temperature due to hydration was predicted with the help of a software program called “KINTEMP”.

## 2 Experiments

### 2.1 *Experimental setup*

The H-shaped concrete specimen has a length of 170 cm and a width of 40 cm and a constant thickness of 5 cm. The notches have a length of 150 cm and a width of 10 cm. In the notches steel tubes with steel plates were inserted as counterfort. The concrete specimen has a double symmetry. It was stored on a wooden formwork panel with a thickness of 17mm. The upper surface of this formwork panel was covered with foil before casting in order to avoid adhesion of the concrete.

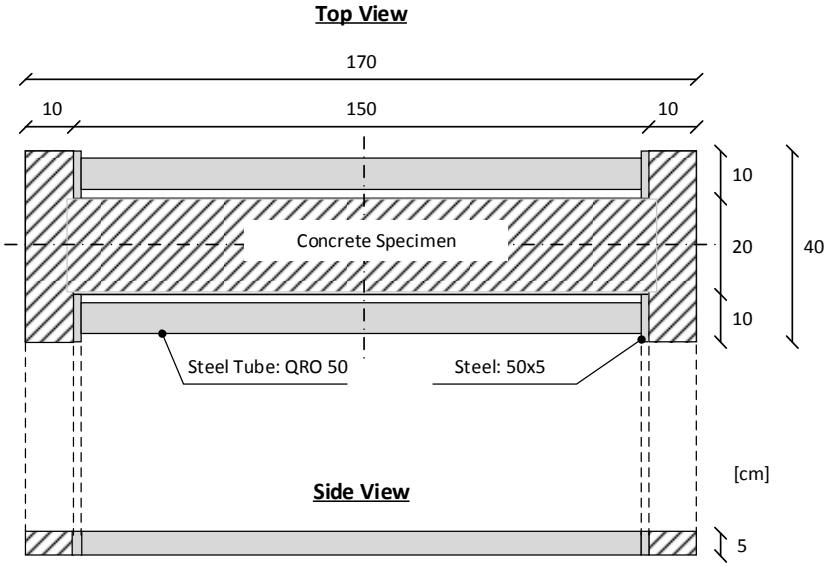


**Fig. 1** Drawing of Concrete Specimen

On both ends of the specimen aluminium elbow were affixed to measure the displacement at the top ends of the specimen with the help of displacement transducers. Under the condition that the steel tubes act as unmovable supports, the displacement transducers measure the deformation of the head parts of the specimen. On the other side to guarantee that the steel tubes act as such a counterfort, the steel tubes were equipped with strain gauges to insure that they do not deform under shrinkage stress.

**Fig. 2** Concrete specimen

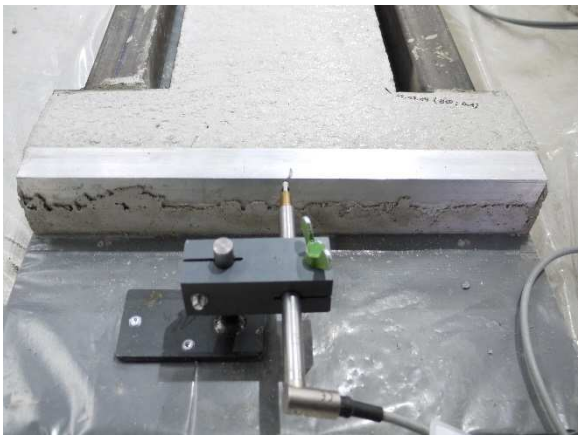

**Fig. 3** Position of the displacement transducer

## *2.2 Testing procedure*

After pouring the H-shaped concrete specimen were stored in a climate chamber. In addition concrete cubes and cylinders were casted in order to analyse compressive strength and elastic modulus evolution. These elements were stored in the same climate chamber where temperature and humidity were kept constant at 20°C and 50% (rel. humidity). The compressive strength evolution was determined by the first day, second, seventh and 28th day measurement.

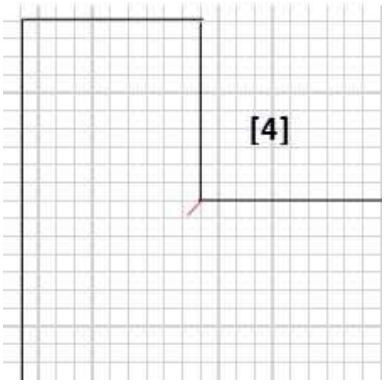


**Fig. 4** Five days

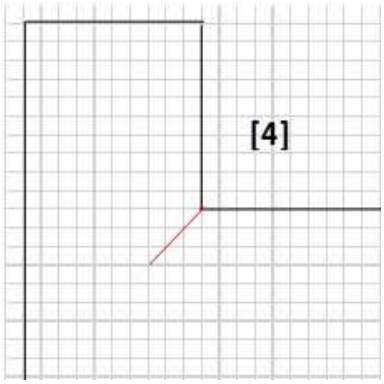


**Fig. 5** Eight days

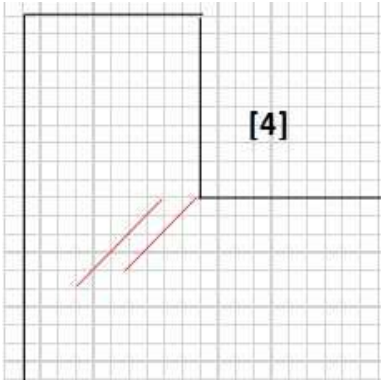


**Fig. 6** Twelve days

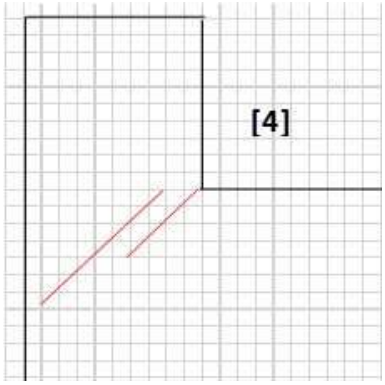


**Fig. 7** 14 days

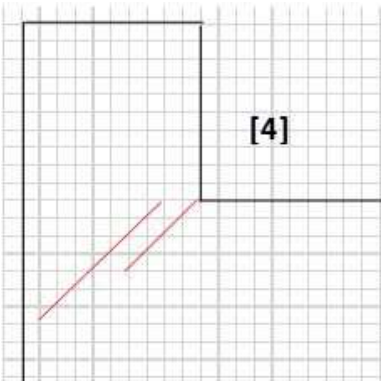


**Fig. 8** 22 days

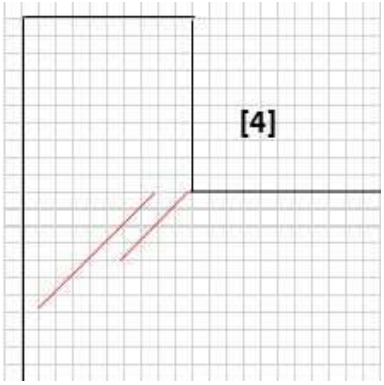


**Fig. 9** 26 days

## *2.3 Test results*

The crack initiation and crack development (length and width) was visually controlled using a scale loupe twice every day and was documented with the help of scale paper. The cracks are exemplary shown for one corner of the specimen in the Fig. 4 to Fig. 9. In addition the amount of cracks is depicted (Fig. 10) and their length and width evolution analysed (Fig. 11 and 12). Totally six cracks occurred during testing period. The first cracks appeared two days after pouring. The crack number is constantly increasing and the final crack pattern is reached at the age of about 35 days. But the cracks grew also in length and width. One can recognize that for the majority of the individual cracks their length undergo an evolution up to the 20$^{th}$ day to around 20 mm. Subsequently these cracks are still increasing in length during the whole testing period.

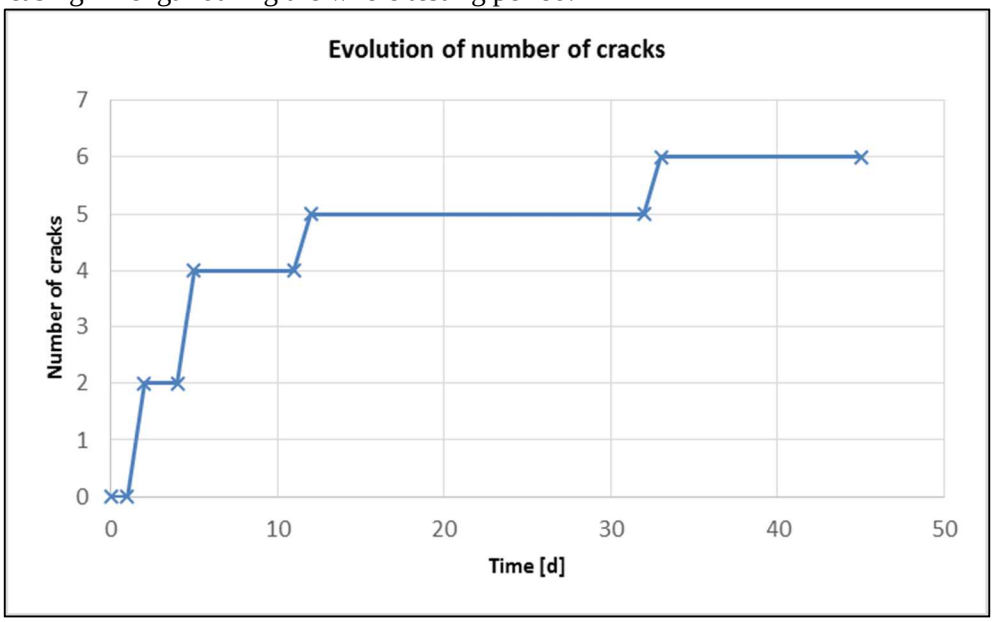


**Fig. 10** Number of cracks

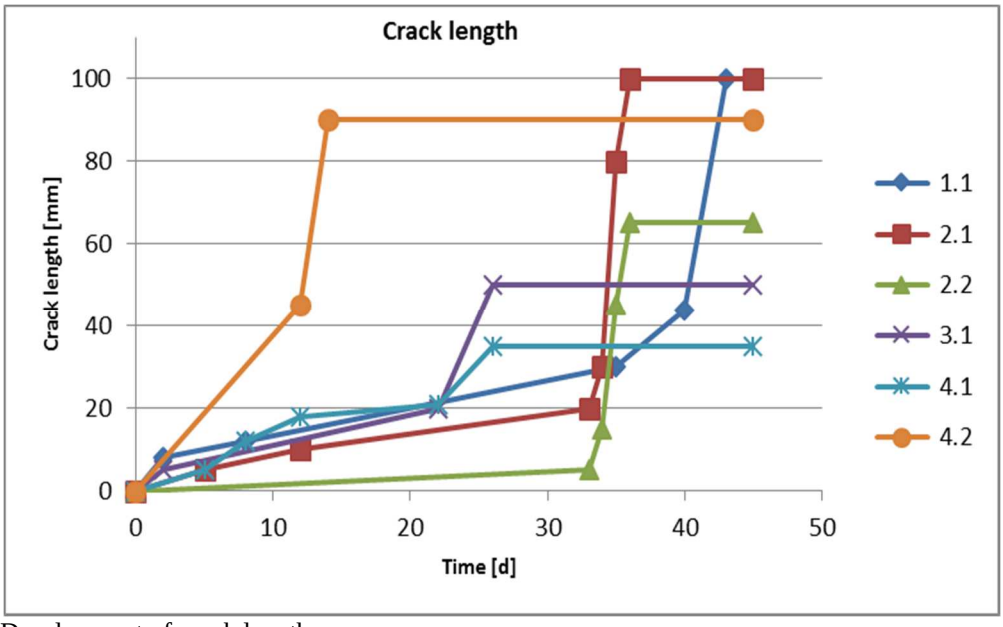


**Fig. 11** Development of crack length

Finally, the crack widths are also registered in their evolution. The smallest cracks visible with a loupe amounted to 0.1 mm. This first cracks occurred after a period of two to twelve days. Until the 45th day, the most of the cracks widened up to 0.2 mm.

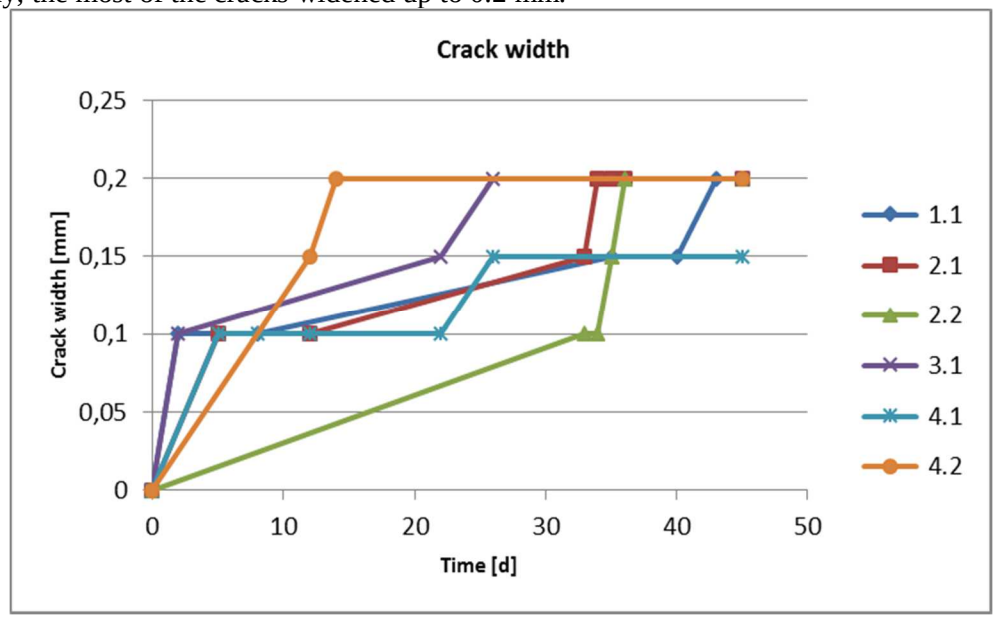


**Fig. 12** Development of crack width

## *2.4 Shrinkage drains*

Three shrinkage drains of the company Schleibinger were filled to compare the measured degree of shrinkage with the analytical approach of the DIN EN 1992-1-1:2011-01. They were stored in a conditioned room and the environmental conditions (temperature, humidity) were recorded over the entire period.

At one end of the drain, a displacement transducer is fixed over a rigid plate to the specimen and records the deformation of the sample every two minutes (Fig.13 and Fig.14).

As a result one can see that the measured shrinkage values (in black) and the calculated degree of shrinkage according to DIN 1992-1-1:2011 EN-01 (in red) presents both a similar behaviour (Fig.15).

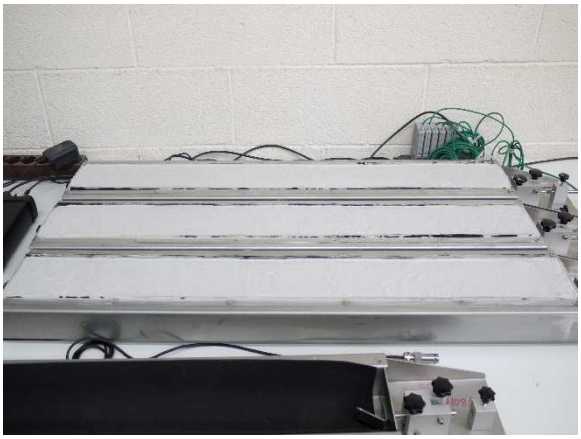

**Fig. 13** Shrinkage drains

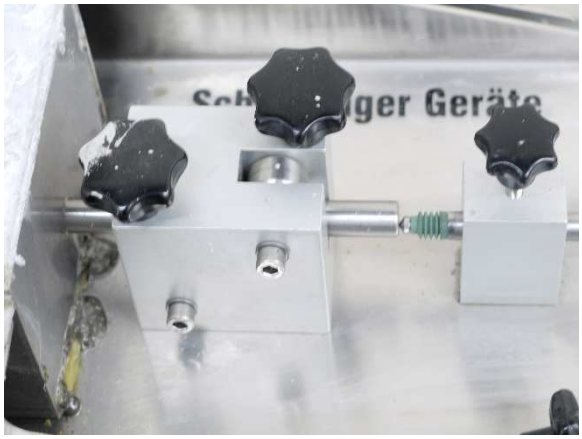

**Fig. 14** Position transducer

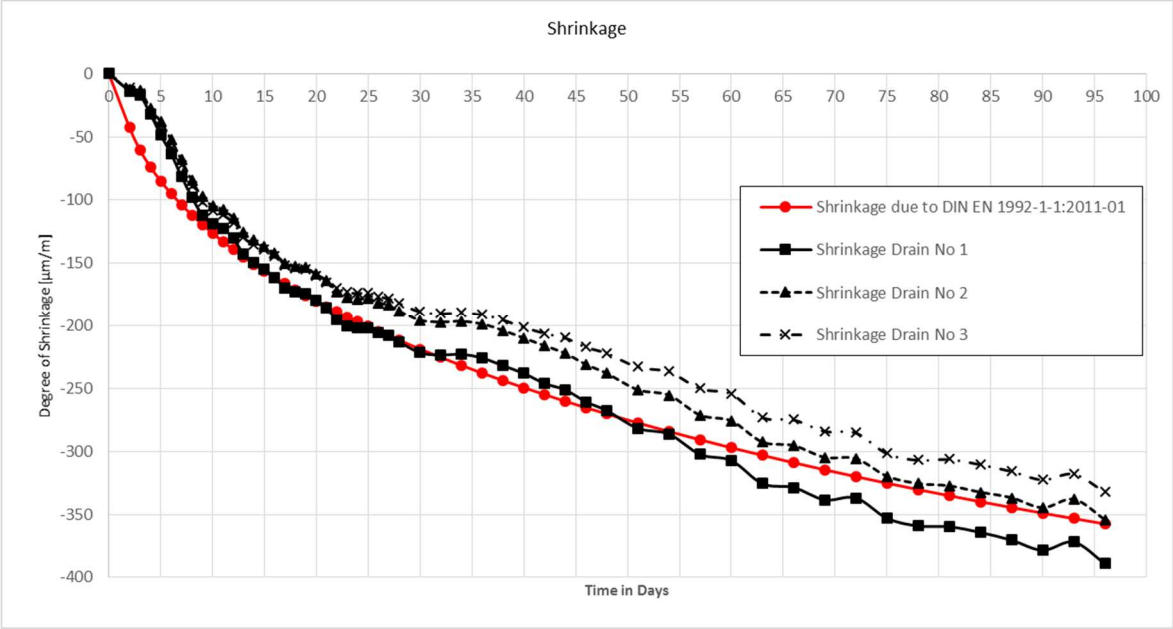


**Fig. 15** Measured shrinkage versus predicted shrinkage

# 3 Finite Elements Model

## *3.1 Aim of simulation*

The findings from the experimental studies are implemented as a result in the finite element program ANSYS. The time and the exact place of cracking, as well as the crack development in the component are simulated by ANSYS. The SOLID65 element is the only element that can represent the formation of cracking by using a non-linear calculation. As a result, it should be possible to make a prediction of crack formation on components with any dimensions.
In addition to the strength and temperature evolutions of the concrete, shrinkage, as a key factor of early stage cracking in concrete, must be represented. A simulation of the shrinkage by applying directly on the element an external strain or tension load case is not possible for the SOLID65element. But in general there is the possibility according to DIN 104:2009-03 to simulate shrinkage by applying a load case simulating cooling of an element. A low temperature is applied to the entire component, while the surrounding environment of the component has a high temperature. This ensures that the component develops strains similar to shrinkage.

To calculate this problem, a thermal loading case is generated for each time step. The cooling temperature is applied according to DIN EN 1992-1-1:2011-01 as this evolution represents with good accuracy the measured values of shrinkage in the shrinkage drains (see chapter 2.4).
Later, the model should be generated via a simple parametric query with regard to length and width of the slab and the edge length of the used element.

## *3.2 Used Prediction Software*

The programs KINTEMP and KINFEST have been developed by Prof. Dr. Gebauer and marketed by COBET Ingenieurbüro Cottbus. The programs serve to predict the temperature (KINTEMP) and strength evolution (KINFEST) of divers' concrete formulations. With the additional module BEPRO concrete formulations can also be optimizes.
KINTEMP estimates the temperature development in structural components, taking into account the formulation, the fresh concrete temperature, the ambient conditions (formwork, air temperature) and

the component geometry. The prediction from the two programs KINTEMP/KINFEST are calculated for a specific well-defined point in the volume (Fig. 17).

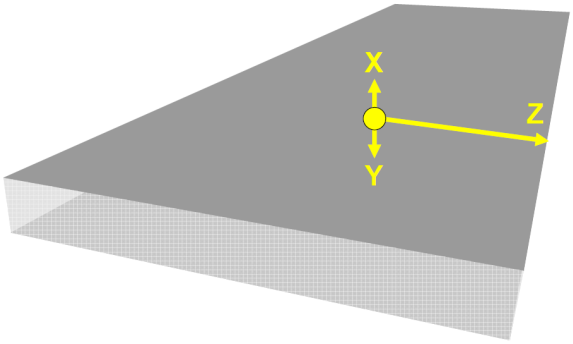


**Fig. 16** Orientation of coordinate system

KINFEST calculates for various concrete formulations and temperature gradients coming out of the program KINTEMP the hardening and strength evolution. This progam has been tested by their developer for nearly all cements and additives, water/cement ratios of 0,20 to 1,00 and concrete voids content from 0 vol% to 12 vol %. Curing times up to 180 days can be represented, as well as concrete temperatures from 0°C to 80°C. So, KINFEST is able to calculates in addition to the evolution of compressive strength, the evolution of the splitting tensile strength, of the bending tensile strength, of the tensile strength and of the E-modulus. The predicted values can be represented in tables and in graphs (Fig. 16).

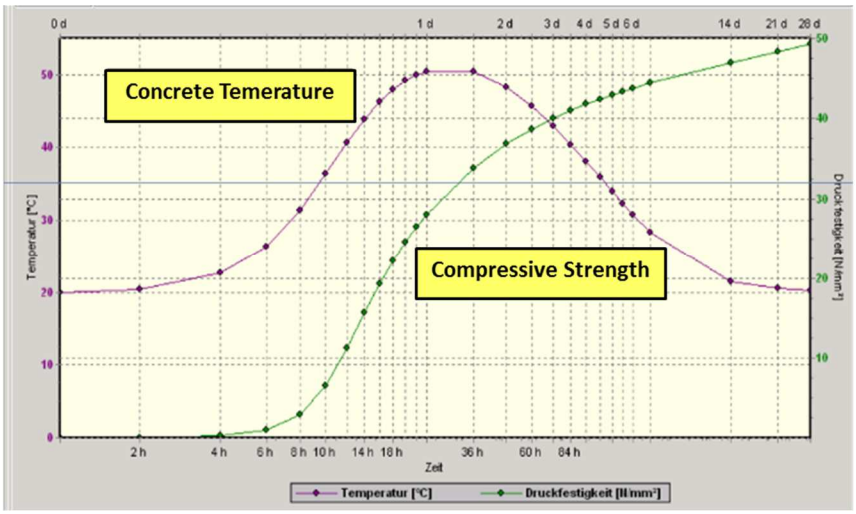


**Fig. 17** Output from KINTEMP/KINFEST

The logarithmic representation of the time axis (X-axis) allows a detailed analysis of the first hours. This is important, because the strength significantly changes in the first hours.
Besides, the heat transfer coefficient and the boundary conditions in function of the formwork (plastic formwork, steel formwork, air) are to take into account.
In the Fig. 18, Fig 19 and Fig. 20 the measured temperature, compressive strength and E-modulus versus the by KINTEMP/KINFEST predicted temperature, strength evolution and the evolution of the elastic modulus are depicted.

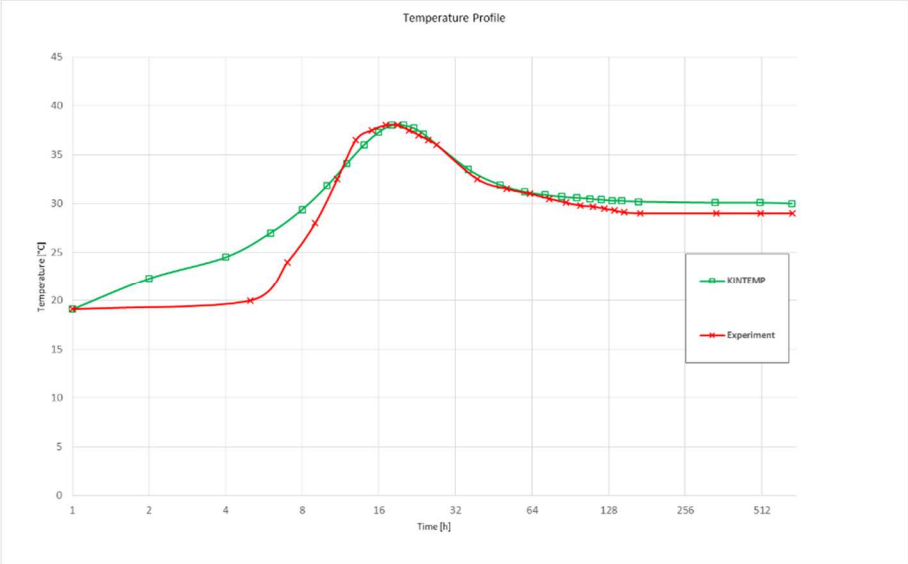


**Fig. 18** Measured temperature versus predicted temperature by KINTEMP

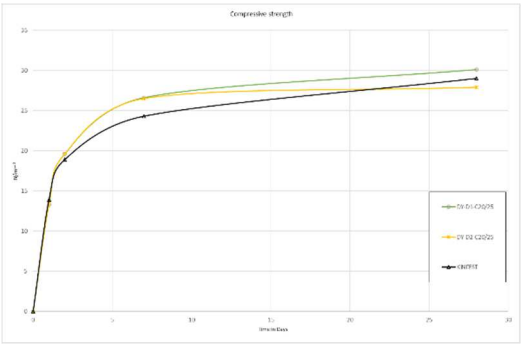

**Fig. 19** Measured compressive strength versus predicted compressive strength by KINFEST

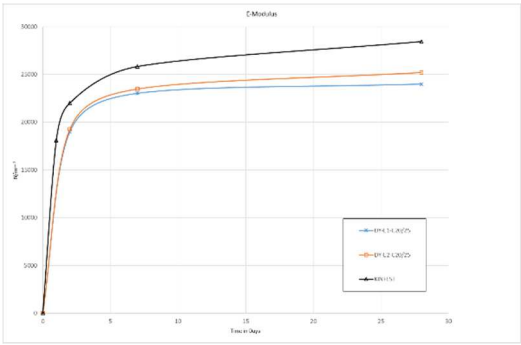

**Fig. 20** Measured E-modulus versus predicted E-modulus by KINFEST

## *3.3 Developed Finite Elements calculation procedure*

### *3.3.1 Description of the Finite Elements Model*

The component geometry has been generated taking into account the symmetry properties. The boundary conditions such as the bearing of the model, the symmetry conditions and strains are set in the next step.

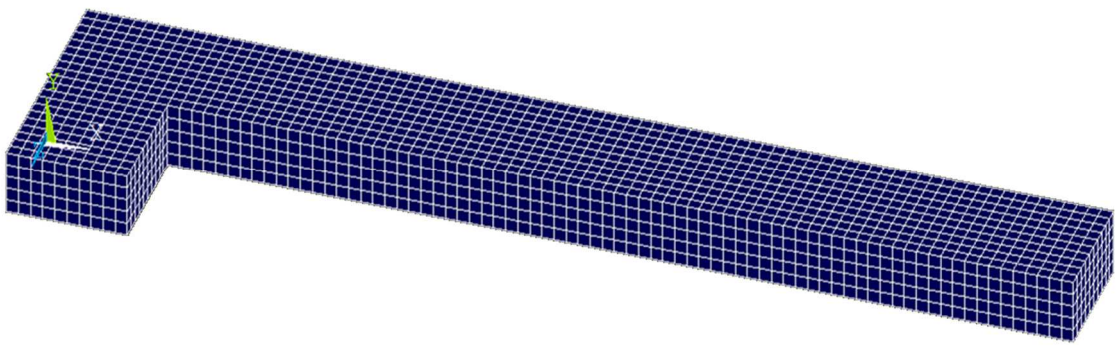

**Fig. 21** Developed Finite Elements Model

*3.3.2 Sequence of simulation*

First of all, the modulus of elasticity, the tensile and the compressive strength arrays are dimensioned. The material characteristic values are delivered by the prediction program KINFEST. Using the example of the young's modulus (*dim,emodul_,array,n,1) it can be understood that a n x 1 matrix is generated where n corresponds to the different time steps during hardening.
Then the required material characteristics from an external .csv file will be read (*vread, emodul_, test_1, csv,,,,,,1).
The now imported values will be modified so that they get a Gauss distribution. This ensures that each element within the component gets a different material characteristic corresponding to a real situation so that by reaching a critical tensile stress not the whole component will crack at once.
With a do loop over the different ages of the component a nonlinear calculation is started and the cracking behaviour evaluated.
In addition, the loop contains the thermal loading case at the relevant age. The thermal loading case is given up as node load on each of the nodes of the model. Starting from the initial defined reference temperature the model receives a cooling, which leads to a contraction of the model according to the shrinkage. The applied temperature according to DIN EN 1992-1-1:2011-01, at the relevant time, is calculated from the calculated degree of shrinkage as follows:

$$\boldsymbol{\varepsilon_{cds} = \alpha_T \cdot \Delta T}$$

$\alpha_T$ = Thermal expansion coefficient
$\Delta T = T_E - T_A$
with: $T_E$ = Last temperature
$T_A$ = Initial temperature

*3.3.3 Results of simulation*

The first time step regarding cracking of the model was t = 12h. The subsequent time steps were for illustration 16h, 18h, 20h, 22h, 24h and also 14 days and 28 days. First the results of the time step t = 28 days is shown (Fig.22 and Fig. 23).

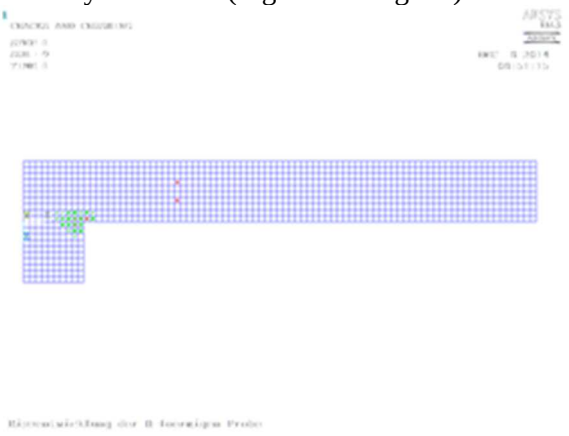

**Fig. 22** Crack formation after 28 days

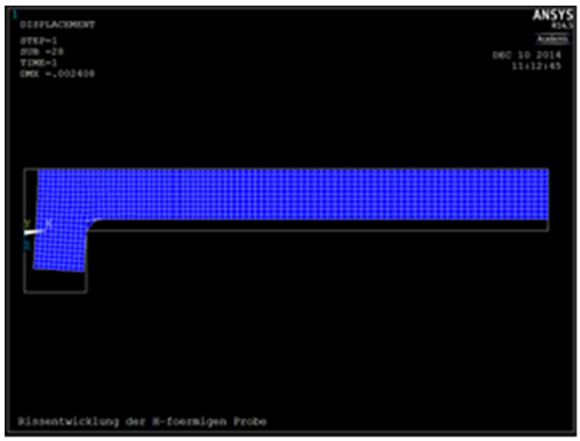


**Fig. 23** Deformation after 28 days

In Fig.24 the cracking corresponding to the time step of t = 28 days, determined by simulation, compared to the cracking at the same age of the experimental specimen is shown. For a better view the cracks at the time step of t = 28 days are drawn in red. It can be stated that the simulation represents the experimental results with very good accuracy.
Crack devolopment from simulaton for all other time steps16 h, 20 h, 14 days and 28 days is shown in the Fig. 25 to Fig. 28.

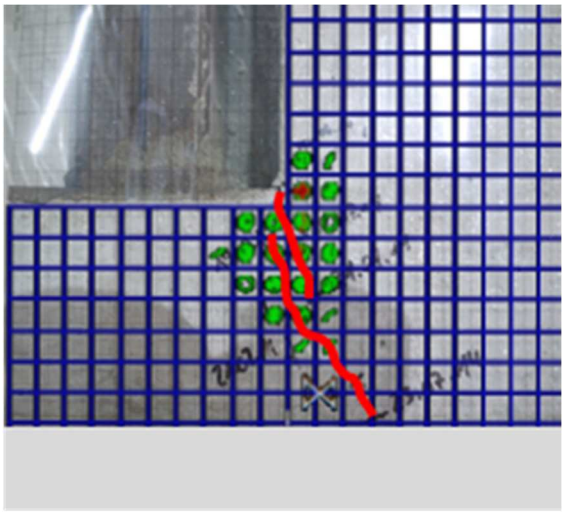

**Fig. 24** Simulated cracks versus measured cracks

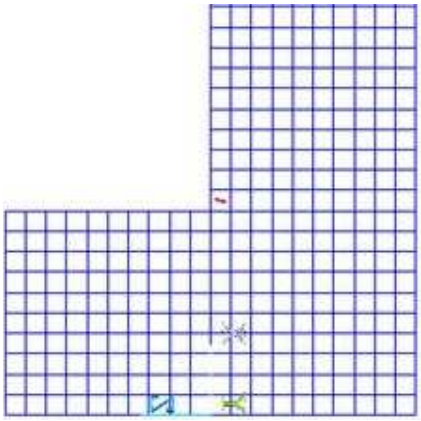

**Fig. 25** Simulated cracks after 16 hours

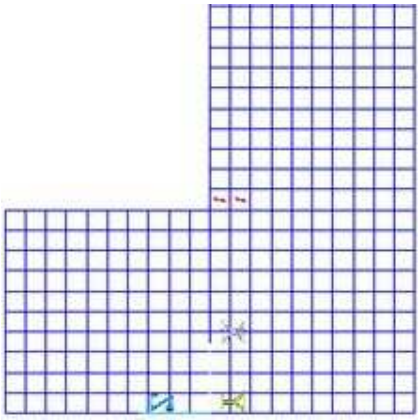

**Fig. 26** Simulated cracks after 20 hours

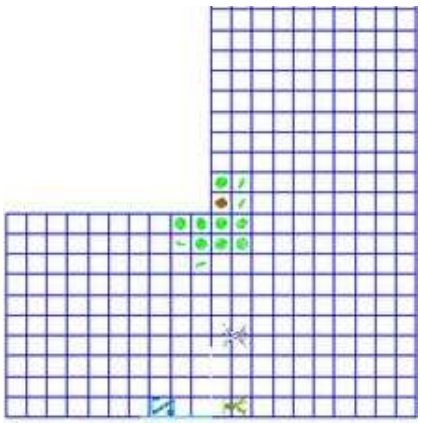

**Fig. 27** Simulated cracks after 14 days

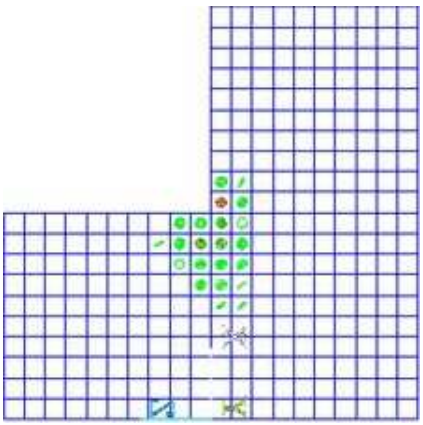

**Fig. 28** Simulated cracks after 28 days

Finally, in Table 1 the actual measured crack lengths are compared to the crack lengths of the FE calculation. A comparison of the values shows that the lengths of the computer simulations are in a same order of magnitude as the crack lengths obtained in the experiment.

**Table 1**

**Measured crack length versus calculated crack length**

| Time step [h/**d**] | Crack length of concrete specimen [mm] 1.1 | 2.1 | 2.2 | 3.1 | 4.1 | 4.2 | Crack length due to FE [mm] |
|---|---|---|---|---|---|---|---|
| | | | | | | | |
| 16 | 0 | 0 | 0 | 0 | 0 | 0 | 10 |
| 18 | 0 | 0 | 0 | 0 | 0 | 0 | 10 |
| 20 | 0 | 0 | 0 | 0 | 0 | 0 | 20 |
| 22 | 0 | 0 | 0 | 0 | 0 | 0 | 20 |
| 24 | 8 | 0 | 0 | 5 | 0 | 0 | 20 |
| **14** | **15** | **10** | **0** | **5** | **18** | **90** | **20-28** |
| **28** | **15** | **10** | **0** | **20** | **35** | **90** | **50-54** |

## 4 Conclusions

The H-shape with the counterforts delivers very good results in terms of crack inition and crack evolution and serves as appropriate experimental setup for the given investigations. Also the degree of shrinkage determined in the shrinkage drains showed a good agreement with the on the basis of DIN EN 1992-1-1:2011-01calculated values.
This FE model is so far developed that any rectangular body can reproduce by introducing some parameters. Shrinkage can be simulated by means of a temperature load case calculation. The material characteristics in function of the strength and temperature evolution are implemented within the FE model by importing data from KINTEMP and KINFEST.
In future the model will be further developed in order to allow a calculation of a complete screeds taking into account beneath of the shrinkage, temperature and strength evolution also the mechanical deformations due to for example bending of the structure.

## Acknowledgements

The experiments were supported by the Wilhelm Dyckerhoff Institute in Wiesbaden (WDI).

## References

Wischers, Manns. Ursachen für das Entstehen von Rissen in jungem Beton. Vortrag auf der Technisch-wissenschaftlichen Zement-Tagung, 21. September 1972, Berlin

Kampen. Risse im Beton: Zement-Merkblatt Betontechnik B18, 2003

Thienel, Kustermann. Sonderbetone- Normalbeton, Hochfester Beton, Hochleistungsbeton, Ultrahochfester Beton. Auszug, 31-33, 2011

Braasch, Buschmeyer. Verbesserte Dauerhaftigkeit: Kontrolle zur frühen Rissbildung. Beton- und Stahlbetonbau, Heft 11, 2006

Li, Nie, Wang. A numerical simulation of the temperature cracking propagation process when pouring mass concrete. Automation and Construction, 37, 203-210, 2014

G. De Schutter. Finite element simulation of thermal cracking in massive hardening concrete elements using degree of hydration based material laws. Computers and Structures, 80, 2035-2042, 2002

G. De Schutter, L. Taerwe. Degree of hydration-based description of mechanical properties of early age concrete. Materials and Structures, 29, 335-344, 1996

Kronlöf, Leivo, Sipari; 1995; „Experimental study on the basic phenomena of shrinkage and cracking of fresh mortar. Cement and Concrete Composites, Vol. 25, No. 8, 1747- 1754, 1995

A.P. Lampropoulos, S.E.Dritsos. Concrete shrinkage effect on the behavior of RC columns under monotonic and cyclic loading. Construction and Building Materials, 25, 1596-1602, 2011

Leemann, Nygaard, Lura. Impact of admixture on the plastic shrinkage cracking of self-compacting concrete. Cement and Concrete Composites, 46, 1-7, 2014

Leemann, Nygaard, Lura. Impact of admixture on the plastic shrinkage cracking of self-compacting concrete. Cement and Concrete Composites, 46, 1-7, 2014

Banthia, Gupta.Influence of polypropylene fiber geometry on plastic shrinkage cracking in concrete. Cement and Concrete Research, 36, 1263-1267, 2006

Banthia, Sappakittipakorn. Toughness enhancement in steel fiber reinforced concrete through fiber hybridization. Cement and Concrete Research, 37, 1366-1372, 2006

Banthia, Nandakumar. Crack growth resistance of hybrid fiber reinforced cement composites. Cement and Concrete Research, 25, 3-9, 2003

Banthia, Sheng. Fracture touhgness of Micro-Fiber reinforced Cement Composites. Cement and Concrete Composites, 25, 251-269, 1996

Yao, Li, Wu. Mechanical properties of hybrid fiber-reinforced concrete at low fiber volume fraction. Cement and Concrete Research, 33, 27-30, 2003

Hsie, Tu, Song. Mechanical properties of polypropylene hybrid fiber-reinforced concrete. Material Sience and Engineering, A 494, 153-157, 2008

State-of-art report prepared by Task Group 8.7. 2013. Code-type models for structural behavior of concrete. Background of the constitutive relation and material models in the fib Model Code for concrete structures 2010. DCC Dokument Competence Center Siegmar Kästl e.K.: Germany

DIN EN 1992-1-1:2011-01: Bemessung und Konstruktion von Stahlbeton- und Spannbetontragwerken - Teil 1-1: Allgemeine Bemessungsregeln und Regeln für den Hochbau. Beuth Verlag. Berlin

DIN EN 12390-3: 2009-07. Prüfung von Festbeton – Teil 1: Form, Maße und andere Anforderungen für Probekörper und Formen; Deutsche Fassung. Beuth Verlag, Berlin, 2012

DIN 1048-5: 1991-06. Prüfverfahren für Beton; Festbeton, gesondert hergestellte Probekörper. Beuth Verlag, Berlin, 1991

DIN EN 12390-6: 2010-09. Prüfung von Festbeton – Teil 6: Spaltzugfestigkeit von Probekörpern; Deutsche Fassung. Beuth Verlag, Berlin, 2010

DIN Fachbericht 104: 2009-03. Verbundbrücken. Beuth Verlag, Berlin, 2009